

EFFECT OF DOPANT CONCENTRATION ON THE  
THERMOLUMINESCENT RESPONSE OF LiF

by

WILLIAM A. MORRISON

B.S., Grove City College, 1973

---

A MASTER'S THESIS

submitted in partial fulfillment of the  
requirements for the degree

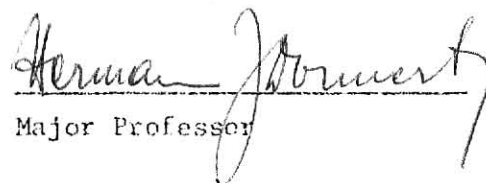
MASTER OF SCIENCE

Department of Nuclear Engineering

KANSAS STATE UNIVERSITY  
Manhattan, Kansas

1975

Approved by:

  
Major Professor

LD  
2668  
T4  
1975  
M68  
C-2

## Table of Contents

1.	Introduction . . . . .	1
2.	Thoery . . . . .	2
2.1	Thermoluminescence (TL) Theory . . . . .	2
2.2	The Crystal Growing Process . . . . .	2
3.	Statement of the Problem . . . . .	4
4.	Description of Equipment . . . . .	5
4.1	Crystal Growing Apparatus . . . . .	5
4.2	Thermoluminescence Readout System . . . . .	13
4.3	Irridation Facilities . . . . .	16
4.4	Lithium Fluoride Crystals . . . . .	16
4.5	Scanning Electron Microscope . . . . .	16
5.	Experimental Procedures . . . . .	18
5.1	Crystal Growing Procedure . . . . .	18
5.1a	Seed Preparation . . . . .	18
5.1b	Charge Preparation . . . . .	18
5.1c	Furnace Preparation . . . . .	18
5.1d	Furnace Operation . . . . .	19
5.2	Readout Procedure for TL Crystals . . . . .	22
6.	Analysis of Data and Results . . . . .	23
6.1	Results from the Readout System . . . . .	23
6.2	Results from Scanning Electron Microgrpahs . . . . .	27
7.	Conclusions . . . . .	37
8.	Acknowledgements . . . . .	39
9.	References . . . . .	40

## Table of Figures

Figure 1.	Crystal Furnace . . . . .	7
Figure 2.	View of Crystal Furnace Internals . . . . .	9
Figure 3.	Crystal Furnace Control Panel . . . . .	12
Figure 4.	Thermoluminescence Readout System . . . . .	14
Figure 5.	Schematic of Thermoluminescence Readout System . . . . .	15
Figure 6.	Portion of WM-2 Crystal . . . . .	17
Figure 7.	Sample Differential and Integral Glow Curves . . . . .	24
Figure 8.	Commercial Pure LiF (Virgin) 30,000 X . . . . .	28
Figure 9.	Commercial TLD-100 (virgin) 30,000 X . . . . .	29
Figure 10.	Commercial TLD-100 (irradiated) 30,000 X . . . . .	30
Figure 11.	WM-1 (irradiated) 30,000 X . . . . .	31
Figure 12.	WM-2 (irradiated) 30,000 X . . . . .	32
Figure 13.	TLD-100 Treatment: Virgin . . . . .	34
Figure 14.	TLD-100 Treatment: 846 krad exposure . . . . .	35
Figure 15.	TLD-100 Treatment: 846 krad exposure, followed by 24 hrs. at 400°C . . . . .	36

## 1. Introduction

As man progresses, he naturally becomes more preoccupied with the quality of his life. This is reflected in the recent criticism of the safety aspects of nuclear power plants. Since the advent of the atomic age, people have been concerned with the effects of ionizing radiation. This concern necessitated the development and refinement of radiation detection and measurement equipment. Daniels [1] first suggested the application of lithium fluoride thermoluminescence for radiation dosimetry work. Some time later the thermoluminescent (TL) characteristics and the value of LiF as a dosimeter became known.

The phenomenon of thermoluminescence is a puzzling thing. Although it has been observed for many years in certain rock samples, the TL mechanism has never been fully understood. If this work can contribute any little piece to the solution of this puzzle, it will have been successful and worthwhile.



## 2. Theory

### 2.1 Thermoluminescence (TL) Theory

A material which stores the energy deposited by incident radiation and subsequently releases it in the form of light when heated is said to exhibit the property of thermoluminescence. These materials are commonly referred to as phosphors. LiF has shown to be one of the more useful phosphors. In its purest form, LiF exhibits very little thermoluminescence. With the addition of impurities, it acquires the characteristics necessary to be an excellent dosimeter. Some of the qualities that make it valuable are: a good energy response (i.e. a linear response over a range of energies) to a variety of radiation types, very little fading (i.e. loss of stored energy or information) of the main dosimetry peaks, and glow peaks whose positions permit easy measurement with modern day equipment.

Despite this knowledge of the characteristics of LiF, the mechanism involved in the TL process is not known. Many theories have been proposed, but none seem quite adequate to fully explain all aspects. A summarization of these theories will not be undertaken here since volumes of literature already exist. The interested reader is directed to consult [2] through [9], and especially [2],

### 2.2 The Crystal Growing Process

The Czochralski technique [10], one of the several widely used and established techniques of crystal growth, was employed. This technique was first applied by Czochralski to metals of low melting point. This method has an advantage due to the fact that it permits the experimentalist to observe the growth process and make appropriate adjustments to insure a good quality product.

There are several main pieces of equipment needed to construct a Czochralski system [10]. A heater assembly with precise temperature control would be the nucleus of such a system. Also needed is a crucible which will contain but not react with the charge placed in it. A charge is that material plus any dopants which are placed in the crucible to be melted and ultimately pulled into a crystal. Another requirement is a seed crystal plus the equipment necessary to manipulate this seed in various manners (i.e. provide rotation and withdrawal from the melt). A seed is a small piece of material, of the same type which is being grown, that is introduced into the melt to provide a surface on which crystallization can commence.

Little information is available on the art of crystal growing. In fact, many consider it a "black art" of sorts. At any rate, the quantitative details of the crystal growth process is left up to the individual grower (i.e. information concerning pulling rates, rotation rates, etc.). The following general discussion may be of some help to the novice, however.

The charge is brought to a temperature slightly above the melting point. The seed is then introduced into the melt and part of the seed is allowed to liquify. The beginning of growth is a critical time and any defects which are initiated at this time can be propagated throughout the remainder of the crystal. The melting of a portion of the seed creates a clean, smooth surface for the beginning of growth and minimizes the defect concentration. Then, the temperature is set in a decreasing mode (i.e. allowed to fall at a slow constant rate) and at the conditions deemed appropriated by the crystal grower, the withdrawal of the seed (pulling) is commenced. The pulling rate, the temperature reduction rate, and the rotation rates (if any) of the seed and crucible are left up to the discretion and experience of the grower. However, it should be noted that these rates are determined, to some degree, by the size and shape of the crystal desired.

### 3. Statement of the Problem

Mohammed Kaiseruddin [2] studied the spectral response of LiF. With the use of a then experimental infrared-sensitive PM tube, he discovered a peak in the thermoluminescence spectrum at approximately  $7450\text{\AA}$  (1.65 eV). This is in addition to the well-known peak at approximately  $4050\text{\AA}$  (3.05 eV). In performing neutron activation analyses on his LiF crystals, he noticed that the ratio of concentrations of the two major dopants, Ti and Mg, was approximately equal to the ratio of the areas under the two observed peaks in the TL spectrum.

Was there indeed a relationship between these ratios? The answer to that question was the objective of this research.

In principle, this would be easy to show. LiF crystals of different dopant concentrations are needed. Since Harshaw Chemical Co., the major manufacturer of TL materials, was unwilling to help in this respect, it was decided that the crystals would have to be grown with the facilities present.

It was obvious from the outset that much material on the subject of crystal growing needed to be assimilated. Also, it became obvious after some experimentation, that much time had to be spent practicing on the crystal furnace here at Kansas State in order to master the general technique of crystal growth and the idiosyncrasies of this particular apparatus.

#### 4. Description of Equipment

##### 4.1 Crystal Growing Apparatus

A vacuum furnace, designated Type No. 2801C, and its accompanying control unit, manufactured by the \*N. R. C. Equipment Corp., was employed in this research. The system, originally designed for growth of silicon rods, was donated to the Chemical Engineering Department by the Western Electric Co. The furnace was then obtained from Chemical Engineering on a semi-permanent basis for this work.

The vacuum furnace consists of a graphite heater coil, quartz heat shields, a graphite crucible and crucible holder, a seed shaft and seed chuck, motors for seed rotation, seed vertical pull, crucible rotation, and crucible vertical lift, suitable connections for vacuum or inert gas operation, water cooling coils, a temperature sensing apparatus, and quartz viewing ports. (See figures 1 and 2)

The control unit consists of a strip chart recorder and its accompanying suppression potentiometers, a voltmeter, an ammeter, a programmer unit, an automatic temperature control interrupter, speed and directional controls for the four motors on the vacuum furnace, and an "Electr-O-Volt" unit. The "Electr-O-Volt" unit permits operation in either the manual or automatic mode. Manual operation gives direct operator control on the furnace power or temperature, while in the automatic mode, the furnace attempts to maintain the temperature set by the programmer unit.

NOTE: The following discussion and numbered items refer to figure 3.

To operate the crystal furnace properly, a knowledge of the functions of the different units comprising the control panel is essential. For this reason, a more in depth description is in order.

\* National Research Corp., Newton, Mass.

Index to Numbered Items on Figure 1

1. Lower half of furnace vessel
2. Upper half of furnace vessel
3. Seed shaft
4. Seed rotation motor
5. Seed vertical pull motor
6. Crucible rotation motor
7. Crucible vertical lift motor
8. "Radiamatic Head"
9. Pressure relief valve
10. Gas Flowmeter
11. Quartz viewing ports
12. Upper cooling loop pressure guage
13. Seed shaft carriage release lever

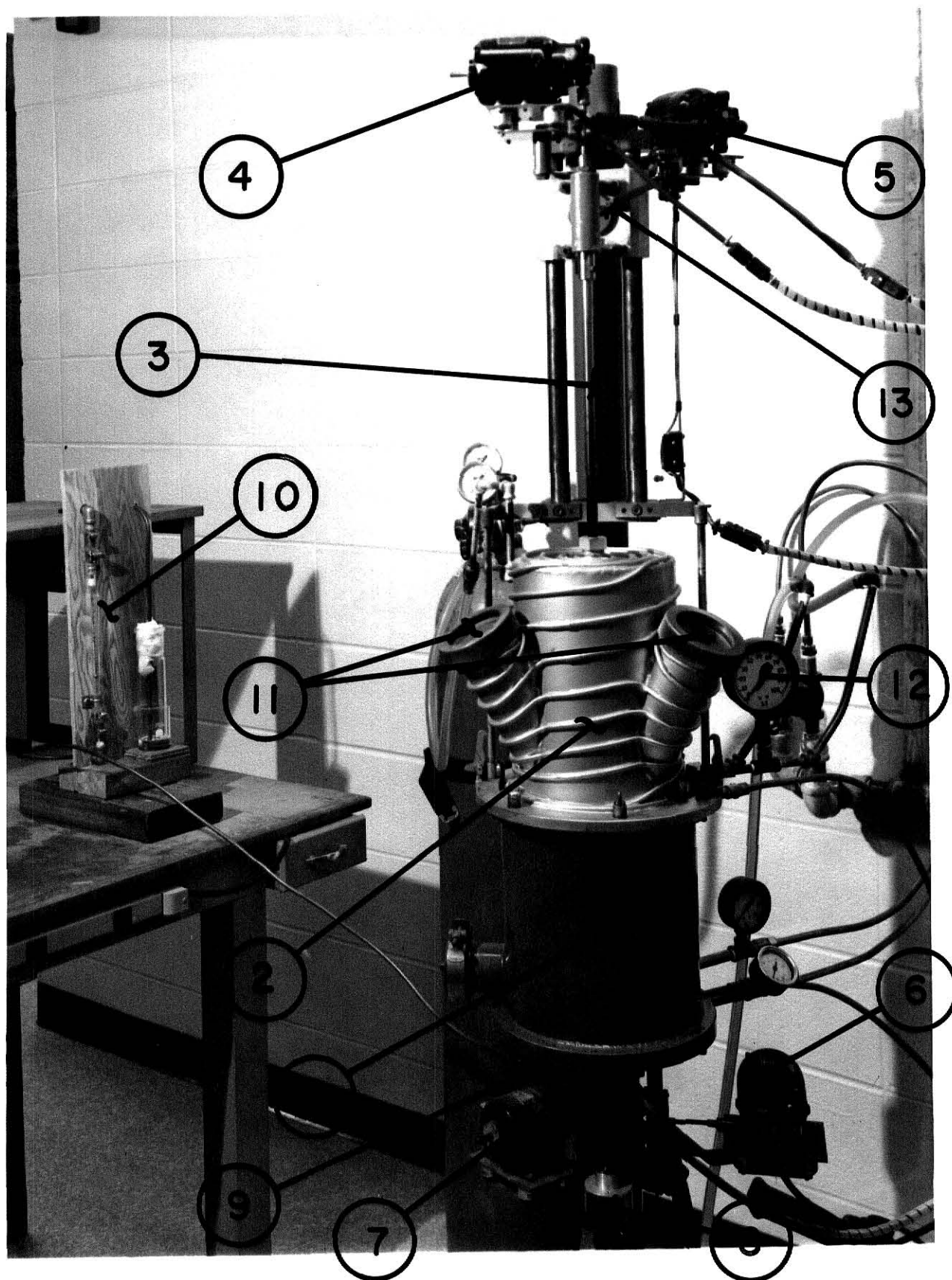


Fig. 1 Crystal Furnace

Index to Numbered Items on Photograph 2

1. Seed check
2. Seed (secured)
3. Lower half of furnace vessel
4. Quartz heat shield
5. Graphite heater coil
6. Graphite crucible
7. Crucible liner

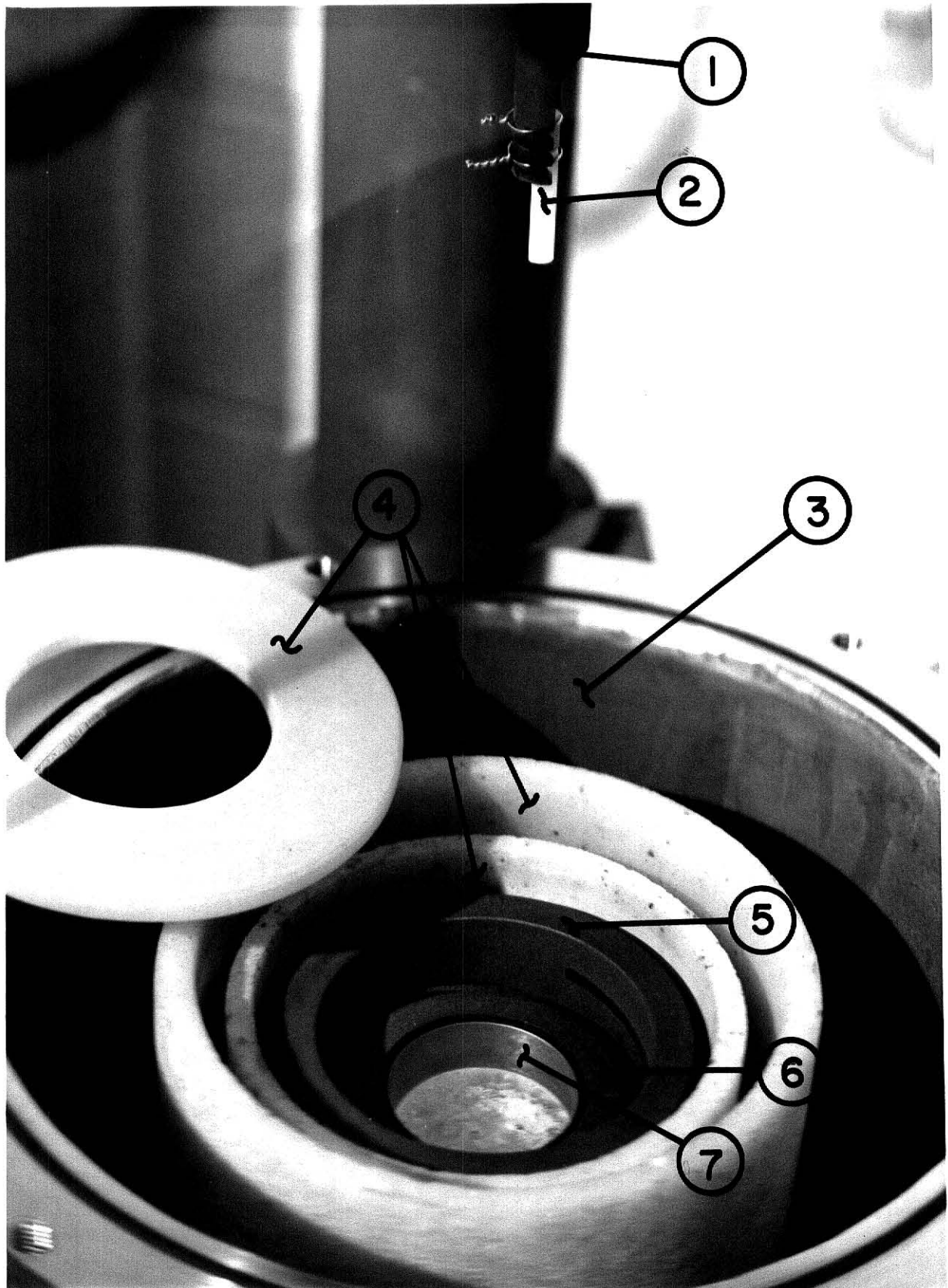


Fig. 2 View of Crystal Furnace Internals



The first thing one notices in observing the control panel is the large strip chart recorder (item 1). Its function is to graphically display the temperature of the furnace. It is calibrated from 0 to 100 in arbitrary units. The absolute calibration of this recorder is determined by its suppression potentiometers (item 2), which modify the signal resulting from the furnace's temperature sensing apparatus, called the "Radiamatic Head."

The next unit, item 3, is the "Electr-O-Volt." It performs two obvious functions: determination of the mode of operation and adjustment of manual mode power. Its not so obvious function is the determination of the magnitude of the error signal when operating in the automatic mode. The error signal is that signal which represents the difference between the actual temperature indicated on the recorder and the desired temperature indicated on the programmer unit.

Items 6 and 7 are the voltmeter and ammeter respectively. Their obvious functions are to monitor the voltages and currents directed to the graphite heater coil. Due to the insensitivity and inaccuracy of the ammeter, a portable ammeter, manufactured by Daystrom Inc. and designated Weston Model 633, was clipped over one of the current carrying leads to the furnace and consulted during all phases of furnace operation.

The programmer unit, item 8, is calibrated from 0 to 10 which directly corresponds to the 0 to 100 calibration of the strip chart recorder. Its function is to establish the "set point", or temperature that the control system appempts to maintain.

Item 9 is the automatic temperature control (ATC) interrupter. It functions only in the automatic mode and is employed to decrease the power to the furnace during the crystal pulling phase of operation. It is calibrated from 0 to 100 which corresponds to the percentage of time per minute that the set point is being continuously lowered.

## Index to Numbered Items on Figure 3

1. Strip chart recorder
2. Suppression potentiometers
3. "Electr-0-Volt"
4. Mode selection switch
5. Manual power adjustment
6. Voltmeter
7. Ammeter
8. Programmer
9. ATC Interrupter
10. Crucible rotation controls
11. Seed rotation controls
12. Crucible vertical lift controls
13. Seed vertical pull controls
14. Control panel's main circuit breaker
15. Furnace start/stop switch

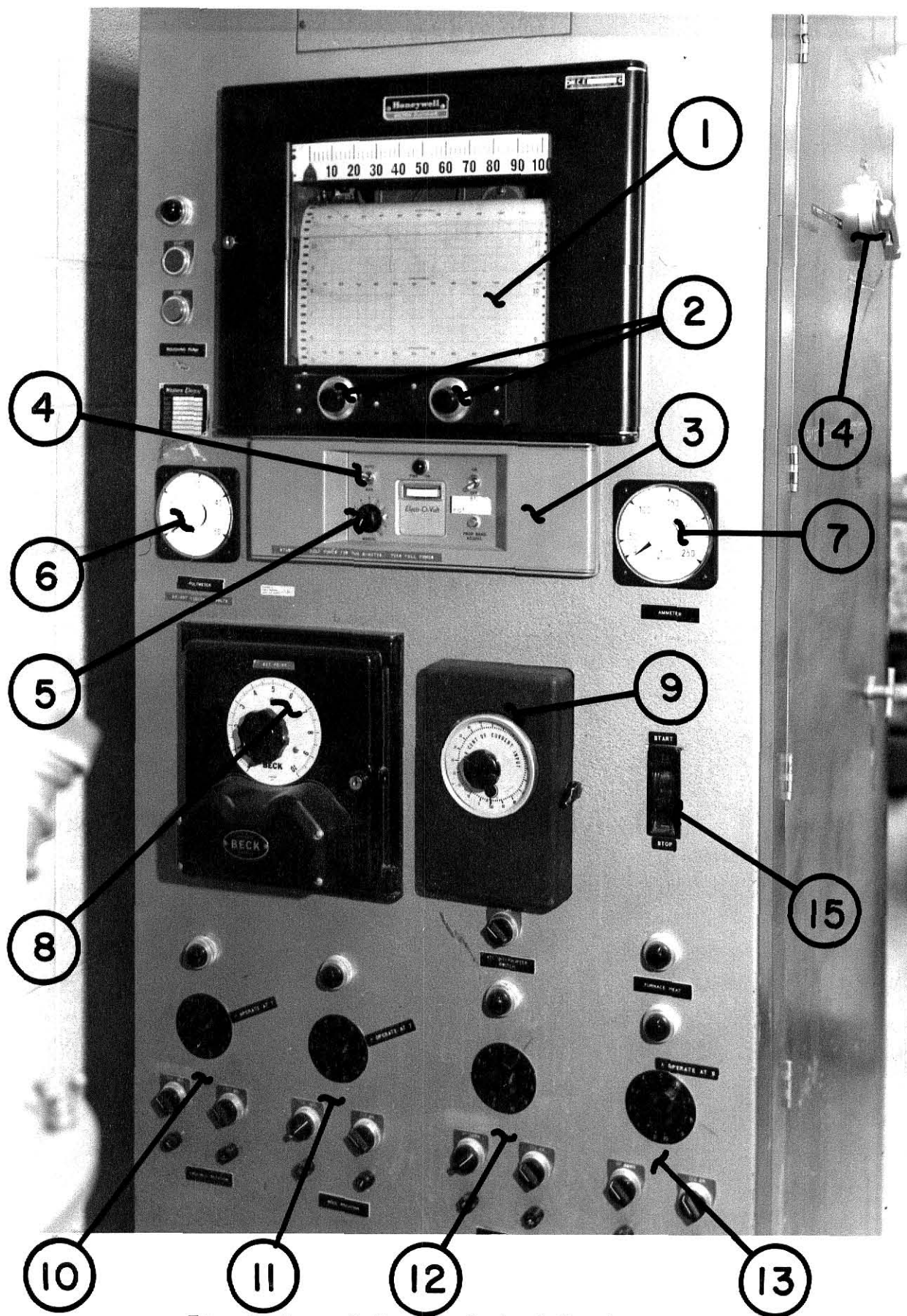


Fig. 3 Crystal Furnace Control Panel

Items 10 through 13 are speed and directional controls for the four furnace motors mentioned previously.

For additional information about the furnace or its control system, consult [11] and [12].

#### 4.2 Thermoluminescence Readout System

The thermoluminescence readout system assembled for this work was essentially the same system employed by M. Kaiseruddin [2]. It consisted of a commercial TLD reader system with appropriate modifications and hardware to split the TL emitted by the doped LiF crystals and obtain two glow curves, an integral and a differential.

There were several minor differences between Kaiseruddin's system and the one employed here. A different kind of high voltage supply and alternate model electrometers were used but achieved the same results as Kaiseruddin's system. The additional picoampere source was employed as an aid in neutralizing dark current from the PM tube but in no way did it change the function of the total system. Also a different type number RCA PM tube was used. It must be pointed out, however, that this PM tube had the same spectral response as did the previous one in Kaiseruddin's system.

Because of the similarities of the two systems, their differences just mentioned being trivial, a more in depth discussion was felt redundant. One is therefore directed to consult the Ph.D. dissertation of M. Kaiseruddin [2] for more information and illustrations concerning such things as read head modifications, PM tube spectral response curves, a programmer heating cycle plot, and equipment operation conditions and settings. Also, the complete readout system used for this work is shown in figure 4 and schematically in figure 5. More information about particular pieces of equipment in this



Fig. 4 Thermoluminescence Readout System

**THIS BOOK  
CONTAINS  
NUMEROUS PAGES  
WITH DIAGRAMS  
THAT ARE CROOKED  
COMPARED TO THE  
REST OF THE  
INFORMATION ON  
THE PAGE.**

**THIS IS AS  
RECEIVED FROM  
CUSTOMER.**

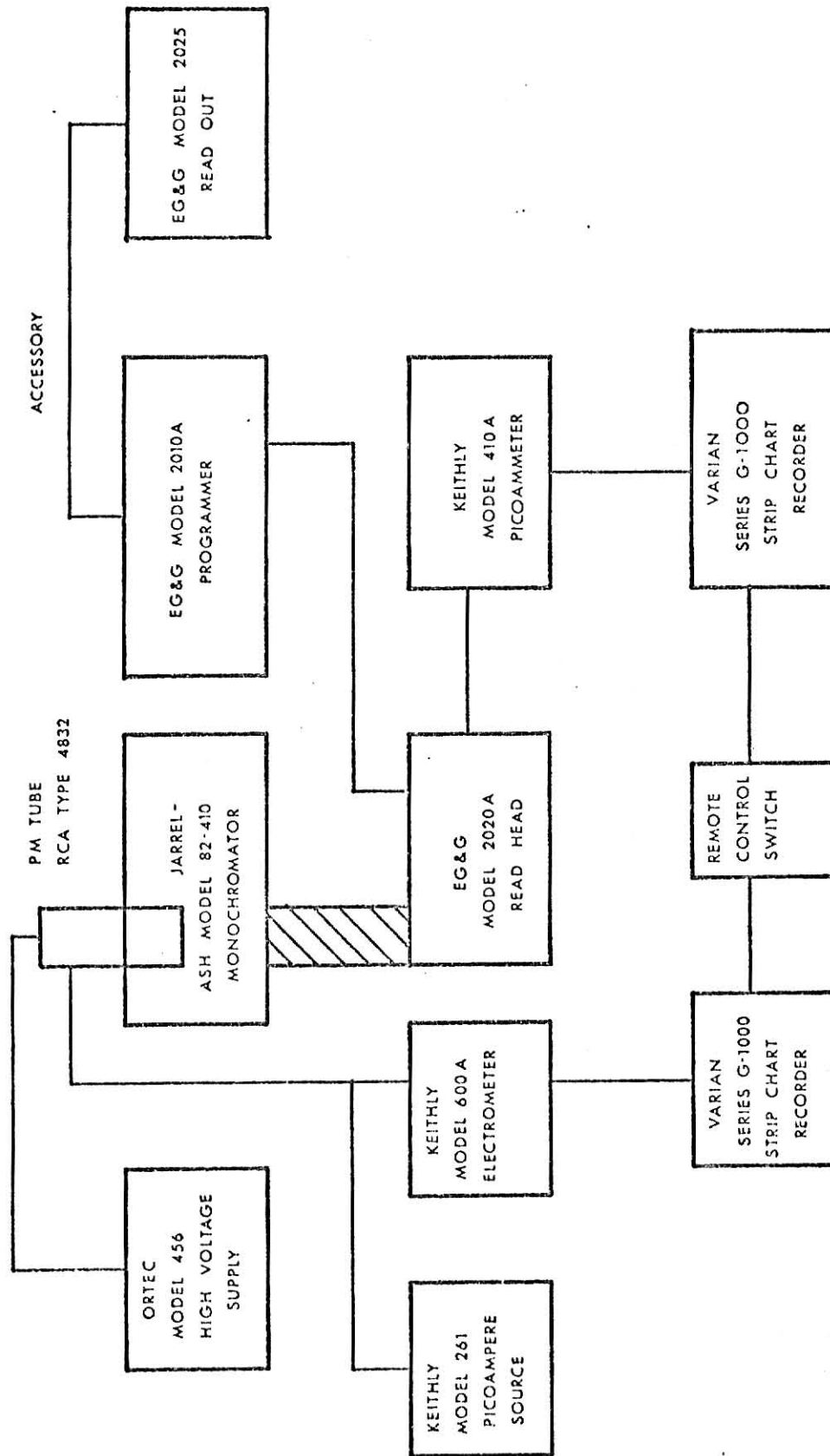


Figure 5. Schematic of Thermoluminescence Readout System



readout system can be obtained by consulting references 13 and 14.

#### 4.3 Irradiation Facilities

LiF crystals were subjected to gamma radiation by employing the KSU Gamma Cell-220 facility. The dose rate was approximately 24 rad/sec at the center of its irradiation chamber at the time when this work was performed.

#### 4.4 Lithium Fluoride Crystals

Two types of LiF TL crystals were used: commercial, TLD-100 manufactured by Harshaw Chemical Co. and those grown with the use of the previously mentioned vacuum furnace.

The two groups of "home-grown" crystals, designated WM-1 and WM-2, were doped with different amounts of titanium and magnesium, which are the two major dopants in TLD-100. Neutron activation analyses (NAA) revealed dopant concentrations of 3.86 ppm Ti and 104.47 ppm Mg in the TLD-100. Similar analyses showed 2.21 ppm Ti, 82.79 ppm Mg, and 4.30 ppm Ti, and 313.49 ppm Mg respectively in the WM-1 and WM-2 groups of "home-grown" crystals.

To obtain a usable form, the TLD-100 crystals were cleaved to a size of 1 x 1 x 0.125 cm. The WM-series of crystals were grown in the form of rods approximately 0.75 cm in diameter and 4.0 cm in length. These were cleaved to produce discs of thickness 0.125 cm.

#### 4.5 Scanning Electron Microscope

The scanning electron microscope located in the Entomology Department was used to study the fine structure of the LiF crystals. This facility provided micrographs of crystal samples at a magnification of 30,000 times and with a resolution of 100 Å.



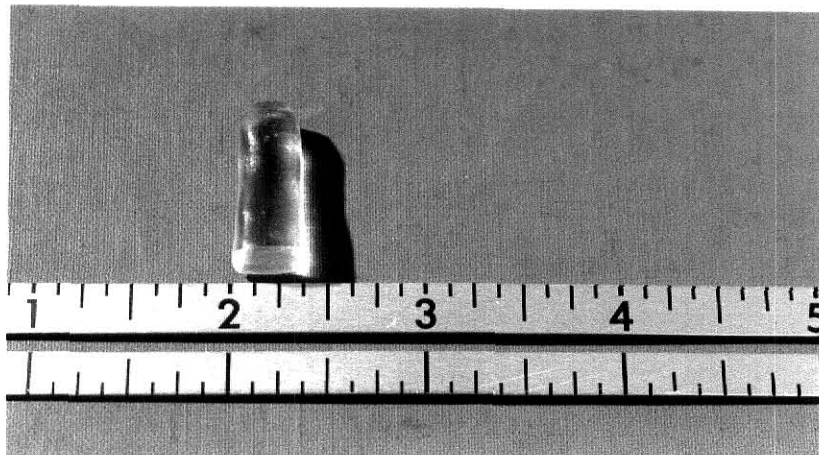
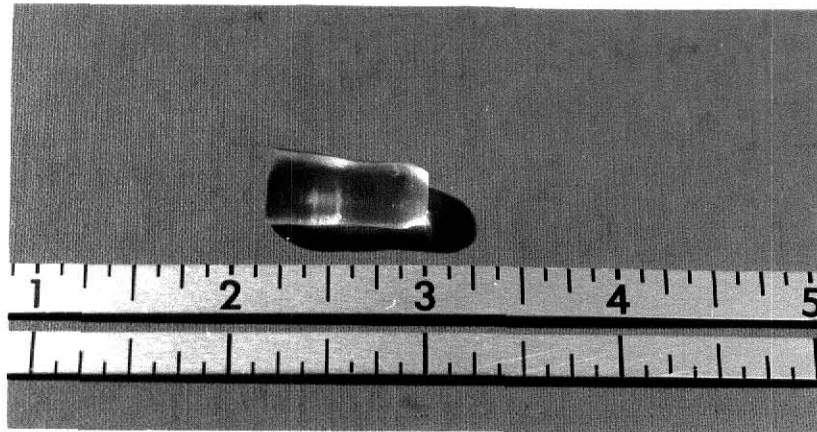


Fig. 6 Portion of WM-2 Crystal

## 5. Experimental Procedures

### 5.1 Crystal Growing Procedure

It should be pointed out that the technique of crystal growing is about as much an art as it is a science. It is a technique which must be developed through practice and patience. The following discussion describes the steps followed during this research. These steps would be similar for all Czochralski type furnaces. For more information, consult references 10, 11, and 12.

#### 5.1a Seed Preparation

Seed crystals were obtained from Harshaw Chemical Co. These came in the form of machined, pure LiF rods 0.2 inches in diameter and 2.5 inches in length. The seed rods were then cleaved in half, perpendicular to an axis running along their lengths. Three notches were scratched into each half-rod near one of the ends. This was accomplished with the use of a jeweler's file. The spacing of the notches on the seeds was such as to match the spacing of the three grooves machined into the seed chuck. See figure 2.

The seeds were then etched in a solution of 1 part HF and 5 parts  $\text{HNO}_3$  and subsequently dried under an infrared lamp. This was done to remove impurities from the surface of the seeds.

#### 5.1b Charge Preparation

Pure LiF, in the form of miscellaneous sized chunks, was ground to a fine powder with the use of a mortar and pestle. The same treatment was applied to the two dopant agents,  $\text{MgF}_2$  and  $\text{TiF}_3$ . The LiF and its dopants were then weighed, mixed, and loaded into a clean crucible liner.

#### 5.1c Furnace Preparation

The furnace internals were cleaned with lintless paper wipes before each

crystal pulling operation. To accomplish this, the wing bolts securing the two halves of the furnace were removed and the top half raised.

Next the notched seed rod was attached to the seed chuck with nickel-chromium wire. Wire was looped around the seeds at the notched positions and then through the grooves in the seed chuck. Finally, the wire ends were twisted until the seed was secured firmly.

Finally, the top half of the furnace was lowered and the wing bolts re-inserted to a finger-tight situation.

#### 5.1d Furnace Operation

The furnace was operated in the inert gas mode using nitrogen. To accomplish this, the pressure relief valve, located on the underside of the furnace was opened. Next, the valves on the gas supply were opened and adjusted to provide a flow rate of 20 CFH. The furnace was purged for about 10 minutes before reducing the flow rate to 10 CFH. \*

During the purging process, the water to the cooling loops was released. Pressure to the top cooling loop, located around item 2 in fig. 1, was adjusted to about 50 psi. Only a trickle of water was permitted to flow in the other two loops, obscured by item 1 in fig. 1. Further adjustments of the cooling water flows were performed during the crystal pulling phase of operation. These were done in an attempt to maintain the furnace's outside surface near room temperature

Following the completion of the purging process, the control panel's main circuit breaker was placed to the "on" position. Next, the strip chart recorder and the "Electr-0-Volt" unit were made operational. The

\* The pressure relief valve is designated item 9 in figure 1.

"Electr-0-Volt" was placed in the manual mode, with manual power at zero, and given several minutes to stabilize. Also, the strip chart recorder's potentiometers were set to zero and not changed. Then, the furnace's start/stop switch was placed in the "start" position. This supplied approximately 60 amps to the heater coil. The crucible rotation controls were set as follows: Speed-5, Direction-forward. Finally, the crucible was lowered to a depth of about .25 inches below the top of the heater coil with the use of the crucible vertical lift controls.

The furnace was allowed to heat at this reduced power level for 5 minutes at which time, full power was supplied. Full power, about 105 amps, corresponded to 10 on the manual power adjustment scale. At this power level, meltdown time of a typical 150 gram charge of LiF was in the neighborhood of 15 minutes. As total meltdown approached, heater current was reduced slightly to prevent overheating of the melt.

When the charge achieved a completely liquified state, the temperature was reduced to find the freeze point. This typically occurred near 40 as indicated by the recorder. To perform this temperature reduction process, the following steps were taken. The programmer's "set point" was placed at 5 and the "Electr-0-Volt" was placed in the automatic mode. This allowed the temperature, as indicated by the strip chart recorder, to fall and approach 50. However, just before the temperature reached that point, the ATC Interrupter was switched on and placed at 2%. This allowed the temperature to be continuously reduced at an extremely slow but fixed rate. When the temperature had fallen sufficiently to produce a frozen crust on the surface of the melt, the ATC Interrupter was switched off and the "set point" was advanced about .2 units. This caused the temperature to be increased such that after several minutes, this crust would disappear and the crystal pulling phase could commence.

The seed was lowered manually until it was just above the surface of the melt. This was accomplished by disengagement of the seed shaft carriage release lever, lowering of the seed, and then the engagement of the same lever. Next, the seed rotation controls were set as follows: Speed-5, Direction-reverse. Then the seed was lowered into the melt to a depth of about .125 inches. This was done with the aid of the seed vertical pull controls. The seed "puddled" for about 10 minutes and after this time, if a clean line existed between the seed and the melt, the actual crystal pulling operation was begun. If this was not the case, the temperature had to be adjusted slightly.

To begin the crystal pulling operation, the seed vertical pull controls were set as follows: Speed-2, Direction-up. The ATC Interrupter was turned on and set to its lowest position (1%). Because the amount of material per unit time being removed from the melt by crystallization during the pulling operation was small, the ATC Interrupter could not be operated continuously. If continuous operation was attempted, the furnace power was driven downscale too rapidly, resulting in a frozen crust on the melt. To prevent this phenomenon, the ATC Interrupter was turned on and off at such intervals as to provide a slight downward trend of the temperature, as indicated by the recorder. Also, there was an attempt made to maintain a constant diameter crystal.

When the crystal had attained the desired length, the seed vertical speed control was adjusted to its maximum (10). This resulted in the withdrawal of the crystal from the melt. The ATC Interrupter was then turned on and set to 10%. This allowed the furnace and crystal to cool gradually. When the heater current reached 60 amps and the temperature leveled out, the furnace's start/stop switch was placed in the "stop" position. The

temperature was allowed to drop below 5 on the recorder before the cooling water and nitrogen gas were shut off. The crystal was not removed until the following day.

## 5.2 Readout Procedure for TL Crystals

The thermoluminescence readout system and procedure used in this work were essentially the same as the ones used by Kaiseruddin [2]. Kaiseruddin was concerned with the construction of a complete thermoluminescence spectrum from 3000 to 8500Å. The scope of this work was confined to obtaining the readings corresponding to those wavelengths (or energies) where the maximums occur in the spectrum. As a result, fewer readings were done.

## 6. Analysis of Data and Results

Although the glow curve of LiF(Tl,Mg) consists of several peaks, only the 210°C peak was analyzed. The heights of this peak were obtained as a measure of the thermoluminescence of the crystals read,

### 6.1 Results from the Readout System

As mentioned previously, both integral and differential glow curves were produced. See figure 7. The differential glow curve (i.e, response from the monochromator and PM tube at a preset wavelength) was normalized by the corresponding integral glow curve. The normalization procedure was used to account for such things as differences in weight of the individual crystals and variations in the irradiation and annealing processes.

At the outset of this research, it was assumed that if crystals of significantly different dopant concentrations were obtained, the object of this work could be accomplished by the mere comparison of the heights of the two peaks in the TL spectrum. Crystals were grown which fulfilled this condition. For this reason, six or more crystals were read at only three or four wavelengths near the maximums of these two peaks. However, the expected significant change in the ratio of these peak heights was not observed. Consequently, for illustration and comparison to Kaiseruddin's [2] data, the following procedure was applied to the raw data obtained.

In this case where the peaks are Gaussian in nature to find the individual peak heights, let:

$$R(E) = R_0 G(E)$$

where  $R(E)$  is the response at energy  $E$ ,  $R_0$  is the peak height, and  $G(E)$  is the

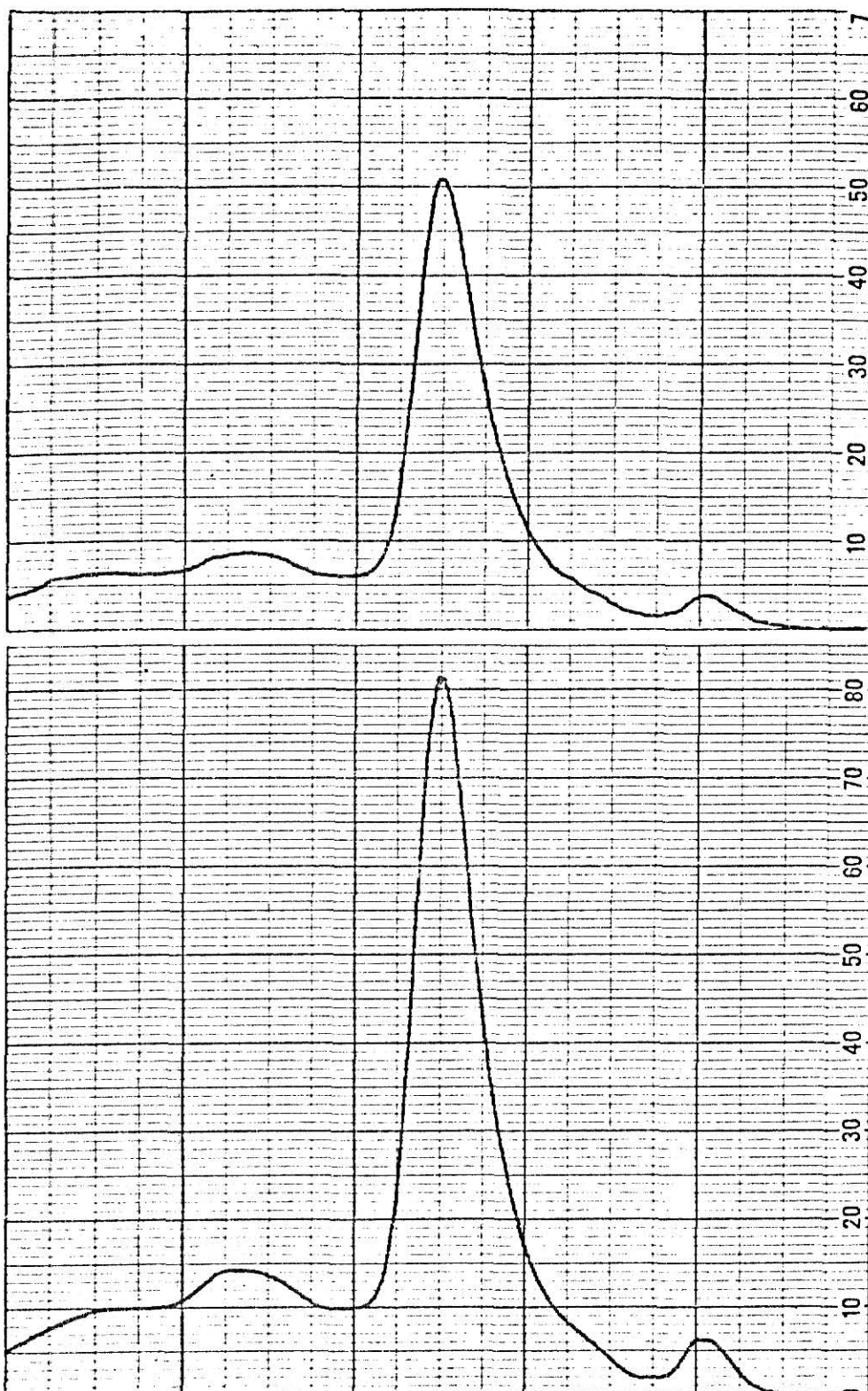


Figure 7. Sample differential (top) and integral (bottom) glow curves.



value of a Gaussian at energy E.

To fit the data points, also assume a weighted least squares fit of the form;

$$\sum_i \frac{1}{\sigma_i^2 \text{ exp}} \{R_i \text{ exp} - R_i(E)\}^2 = \text{minimum}$$

where  $R_i \text{ exp}$  is the experimental response at energy E,  $\sigma_i^2 \text{ exp}$  is the variance on this response, and  $R_i(E)$  is the response at energy E indicated by the corresponding Gaussian fit. The particular fit chosen was performed by Kaiseruddin [2] and designated Figure E-7. This figure is a plot of the Gaussian fit for the TL response at 210°C of TLD-600 exposed to 42.9 krad. The use of this fit was felt justified since the same peak (i.e. glow peak) was studied, the exposure dose employed was 43.2 krad, and the materials analyzed were similar to TLD-600. In reference to the above equation, it should be noted that the summation ranges over all data points collected at each peak in the TL spectrum.

By substituting  $R_o G_i(E)$  for  $R_i(E)$ , differentiating the above summation, and setting the resultant expression equal to zero, the following equation ultimately results:

$$R_o = \frac{\sum_i \frac{R_i \text{ exp} G_i(E)}{\sigma_i^2 \text{ exp}}}{\sum_i \frac{G_i(E)}{\sigma_i^2 \text{ exp}}}$$

The  $G_i(E)$  values are obtained by the evaluation of the following form of the Gaussian expression assuming  $G_{o1}$  equal to one:

$$G_i(E) = G_{oi} e^{-(E-E_{oi})^2/B_{oi}}$$

where  $G_i(E)$  are the intensities or responses at energy  $E$ ,  $G_{oi}$  are the peak heights,  $E_{oi}$  are the peak positions, and  $B_{oi}$  are related to the full widths at half-maximum,  $FWHM_i$ , as:

$$FWHM_i = 2\sqrt{B_{oi} \ln 2}$$

The values of  $E_{oi}$  and  $FWHM_i$  are taken from Kaiseruddin's results for the case in question (i.e. 210°C glow peak, exposure dose of 42.9 krad). The areas under the peaks in the TL spectrum can be calculated as follows:

$$\text{Area} = R_o \sqrt{\pi B_o}$$

The area under peak 2 in the TL spectrum (7450Å) was divided by the area under peak 1 (4050Å) for each group of crystals. These ratios along with the ratios of the concentrations of dopants (Ti to Mg) appear in Table 1. See Section 4.4 for more information about the dopant concentrations.

TABLE 1\*

Crystal Type	Ratio of Peak Areas	Ratio of Dopant Concentrations
TLD-100	0.028 ± 0.001	0.037 ± 0.006
WM-1	0.031 ± 0.002	0.027 ± 0.007
WM-2	0.039 ± 0.003	0.014 ± 0.003

\*Results are for an exposure dose of 43.2 krad.

There was a phenomenon which was observed but not documented that deserves to be mentioned here. A distinct decrease in sensitivity was observed in all three groups of crystals during the repeated irradiations and annealings. Sensitivity, as it is used here, is the measure of the light output per unit

absorbed dose. Due to this curious behavior and to the unexpected results tabulated in Table 1 (the two ratios were expected to behave in similar fashions to the addition of various levels of impurities), it was decided that investigations into the crystal structure needed to be undertaken.

## 6.2 Results from Scanning Electron Micrographs

All micrographs were taken with a sample surface orientation of  $45^{\circ}$  with respect to the electron beam. In the first series of micrographs, Figures 8 through 12, the object was to determine if there were any observable differences between the commercial crystals (i.e. TLD-100) and those grown at Kansas State (WM-series). Figures 8 and 9 are of commercially grown pure LiF and virgin (i.e. unirradiated and unannealed) TLD-100, respectively, both manufactured by Harshaw Chemical Co. They show very little detail except for the presence of several faint lines. These are assumed to be surface defects that were introduced in the cleaving process. These lines were not observed in micrographs of samples with polished surfaces. Figure 10 is of a sample of TLD-100 which had been subjected to repeated irradiations and annealings due to its use in the readout process. It shows a very dense fine structure, some of which appears to be clustering in the form of lines. Figures 11 and 12 are micrographs of irradiated and annealed WM-1 and WM-2 crystals, respectively. They show the fine structure apparent in the irradiated TLD-100. Figure 12 also shows a clustering along lines. The appearance of large, protruding particles in the latter two samples seems to indicate a major difference between these and the previous crystals. The size of these particles is about  $1000\text{\AA}$ . Although the identity of these particles is not known, it is hypothesized that they result from the incomplete melting of dopant materials. This could result from insufficient grinding of the doping agents and/or saturation conditions which are present in the melt.

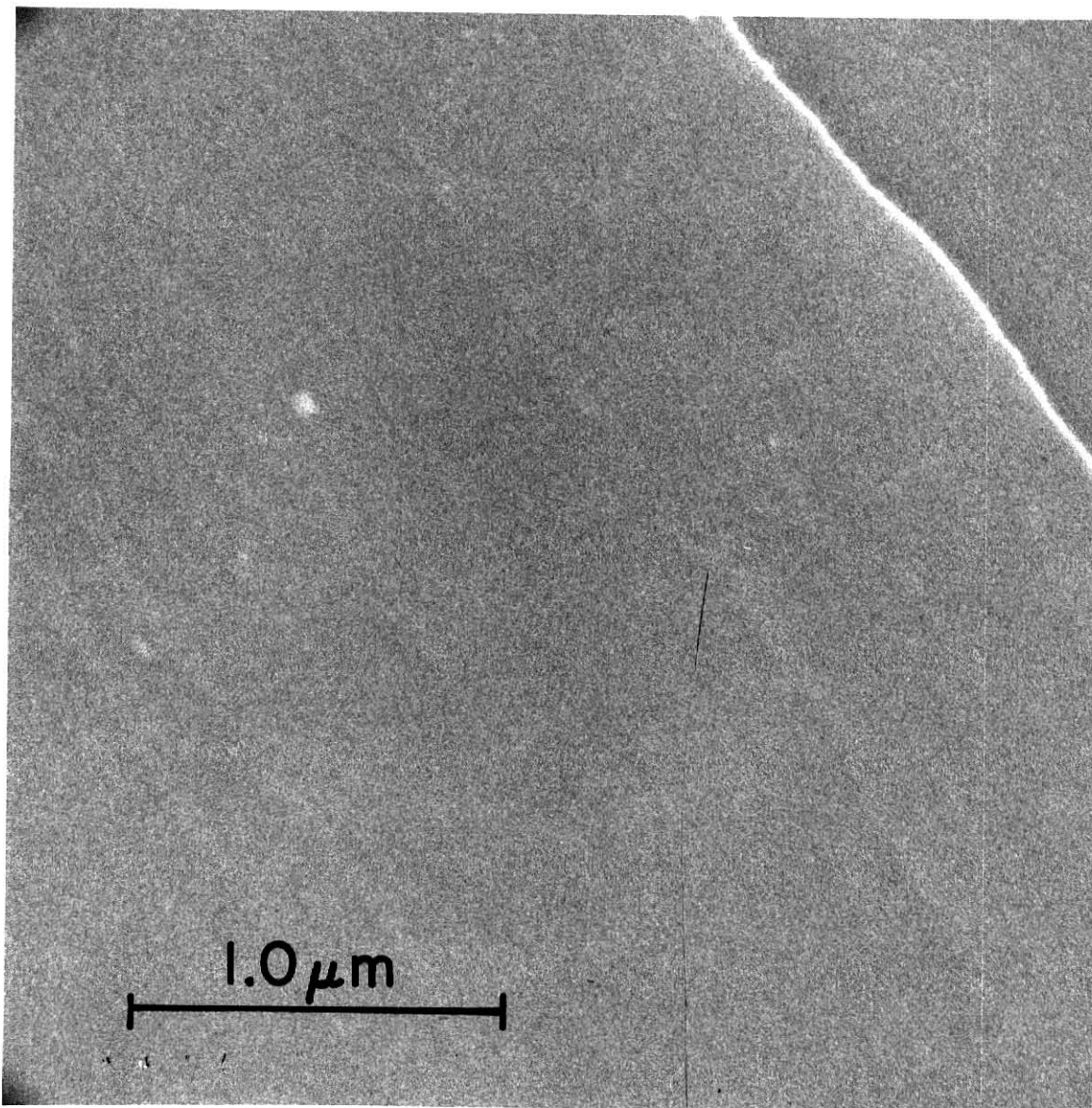


Fig. 8 Commercial Pure LiF (Virgin) 30,000 X

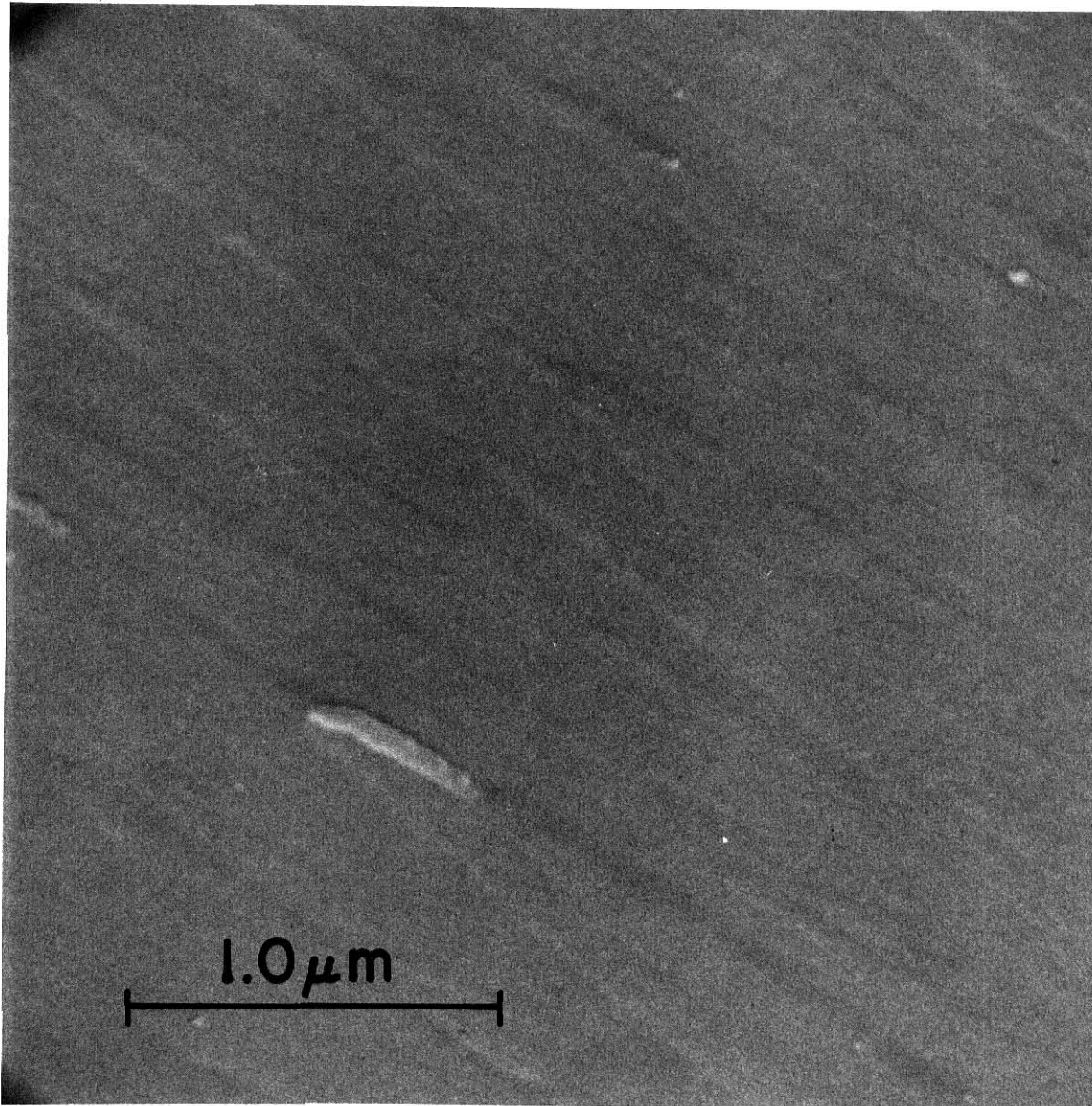


Fig. 9 Commercial TLD-100 (virgin) 30,000 X



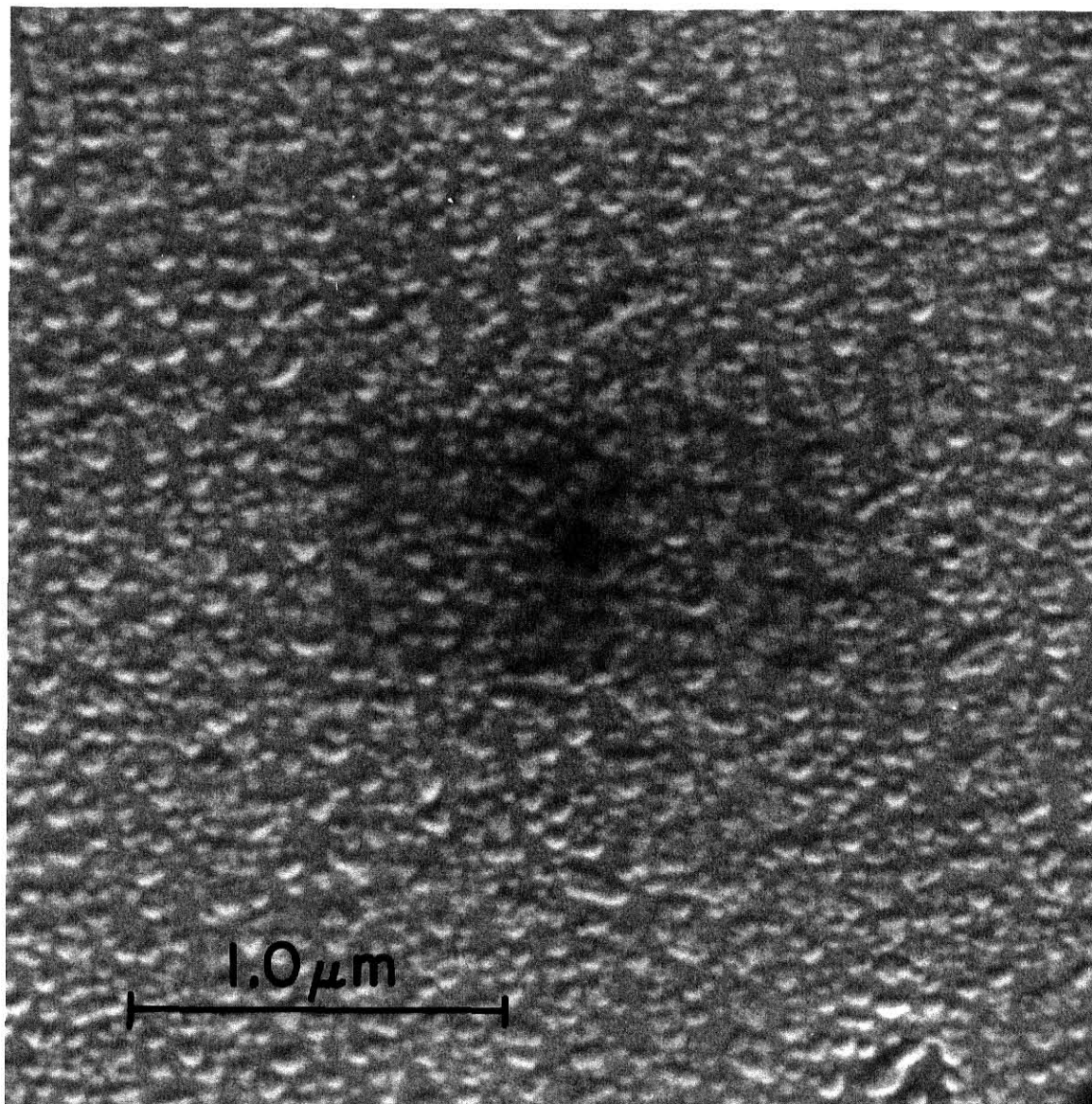


Fig. 10 Commercial TLD-100 (irradiated) 30,000 X

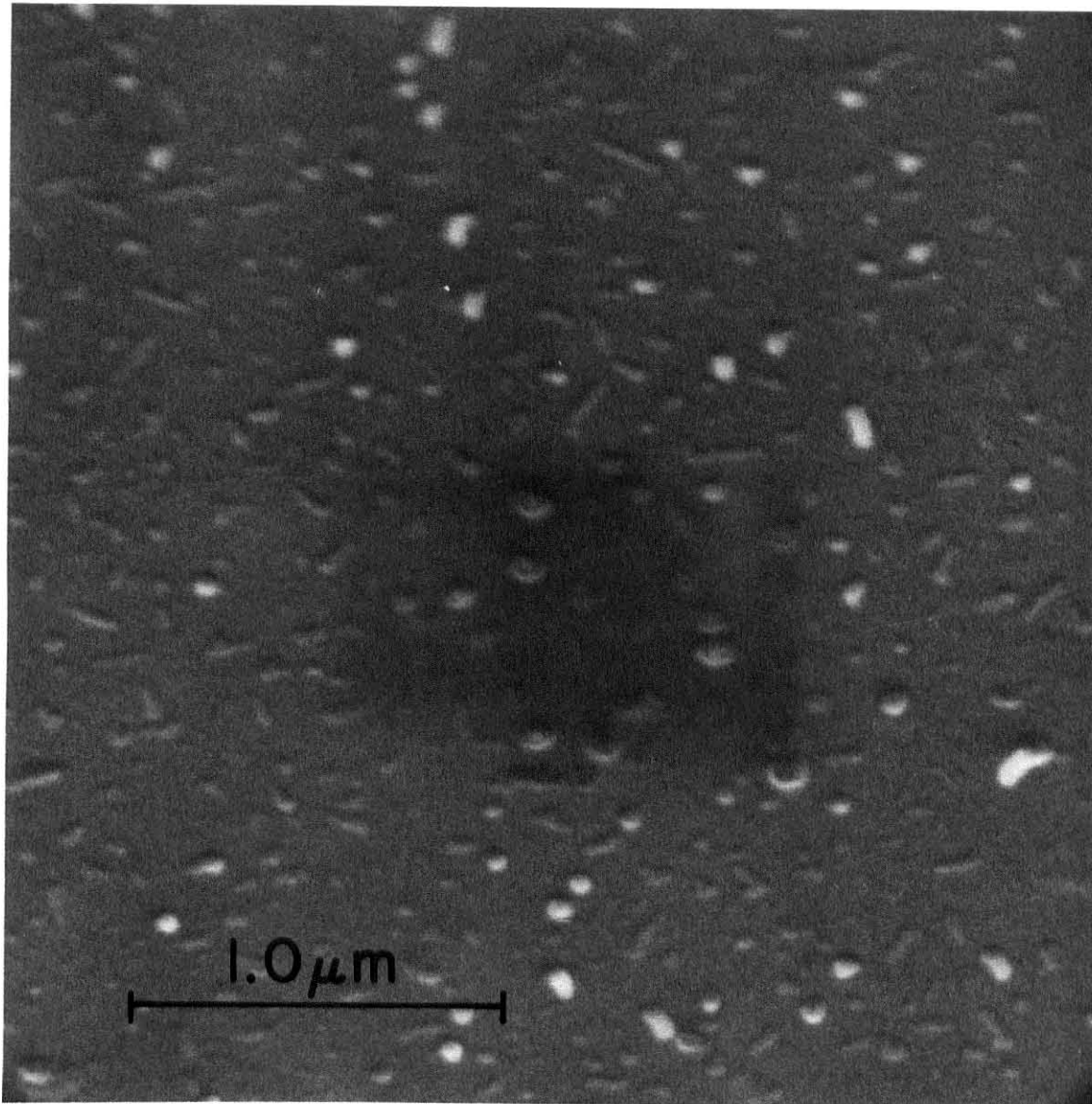


Fig. 11 WM-1 (irradiated) 30,000 X

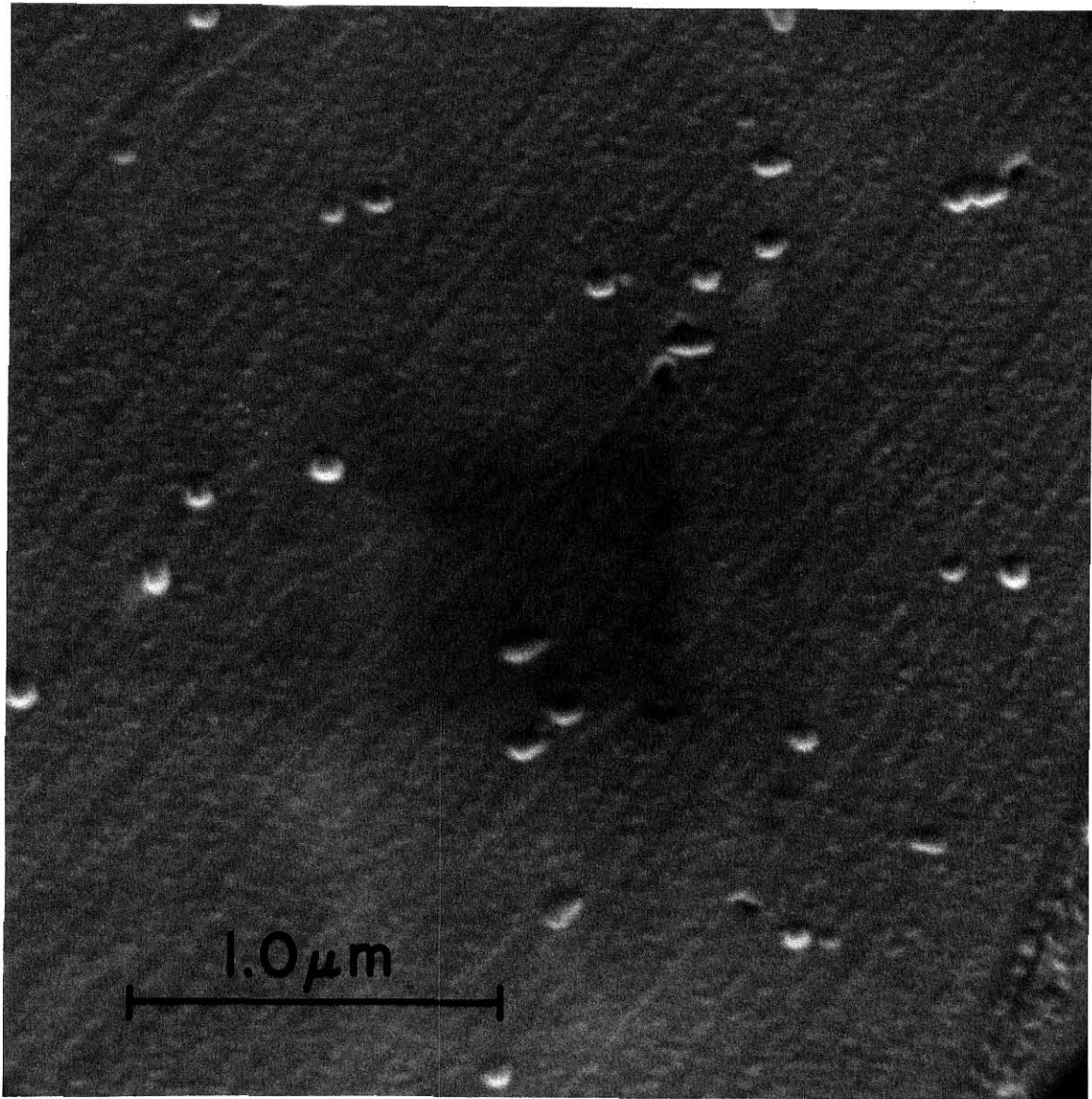


Fig. 12 WM-2 (irradiated) 30,000 X



The second group of micrographs, figures 13 through 15, constituted a brief study of the irradiation and annealing processes (i.e. history) characteristic of the readout procedure and their effect on the fine crystal structure of the TL materials. The crystal samples were cleaved from the same  $1 \text{ cm}^3$  piece of TLD-100. Figure 13, which shows very little detail, is a micrograph of a virgin sample. The crystal illustrated in figure 14 had been exposed to 846 krad of gamma radiation. It shows the presence of fine grain structure and a tendency of clustering in lines prevalent in previous samples. Figure 15 is a micrograph of a sample which had received the same irradiation treatment as did the prior crystal but was annealed at  $400^\circ\text{C}$  (standard annealing temperature for LiF) for 24 hours. It shows considerable roughening of the surface and enlargement of the grain structure. A similar enlargement of grain structure was observed by Gilman and Johnston [15] after the annealing of neutron-irradiated LiF. This behavior seems to indicate that the irradiation process produces defects, which to some degree, are freed in the annealing process and allowed to aggregate or cluster. If the lines appearing on several virgin samples are truly resultant from surface defects initiated in the cleaving process, then it follows that a certain degree of aggregation of crystal defects could occur in these areas of lower energy. This would explain the tendency of the fine structure to cluster in the form of lines.

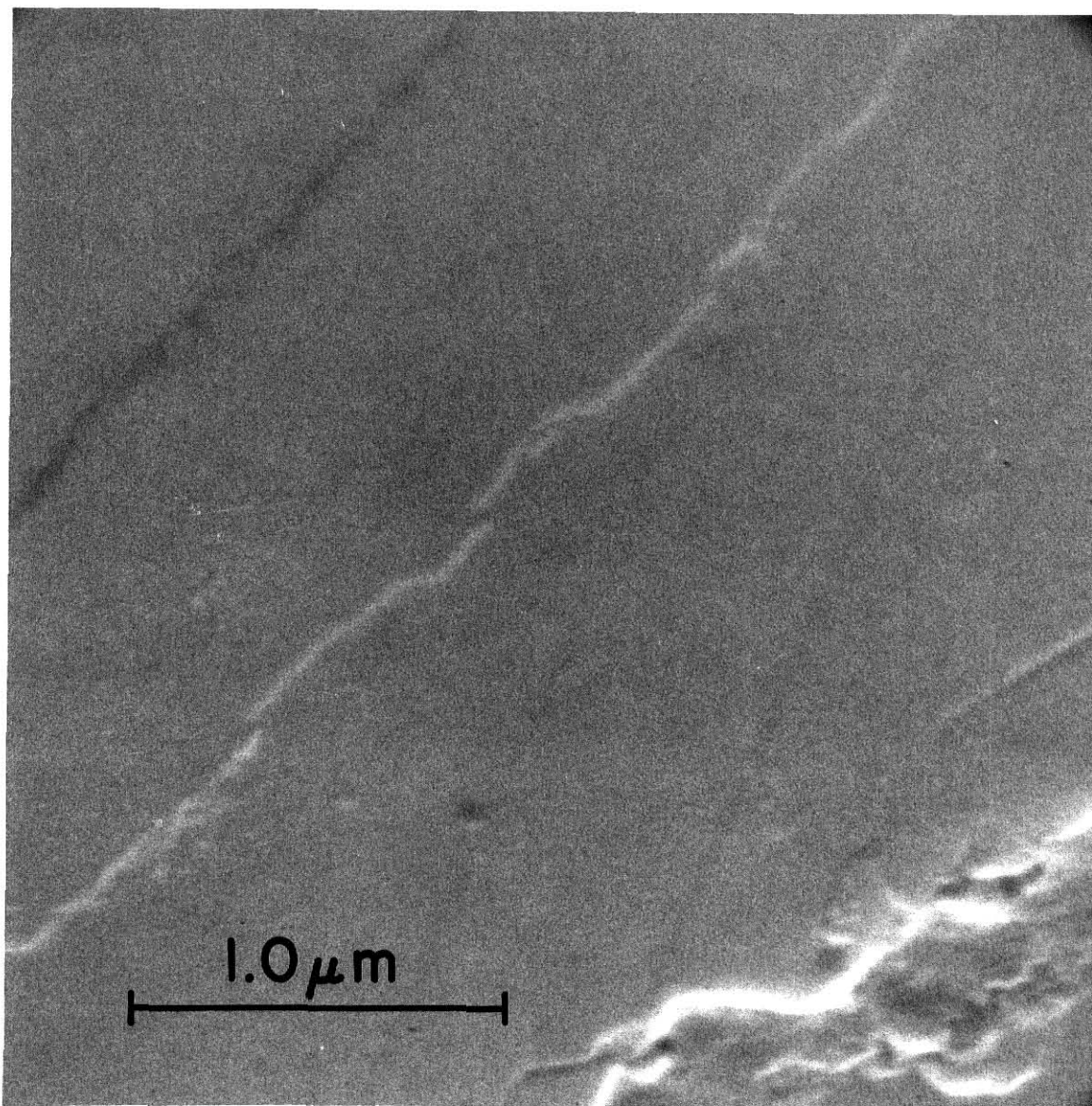


Fig. 13 TLD-100 Treatment: Virgin

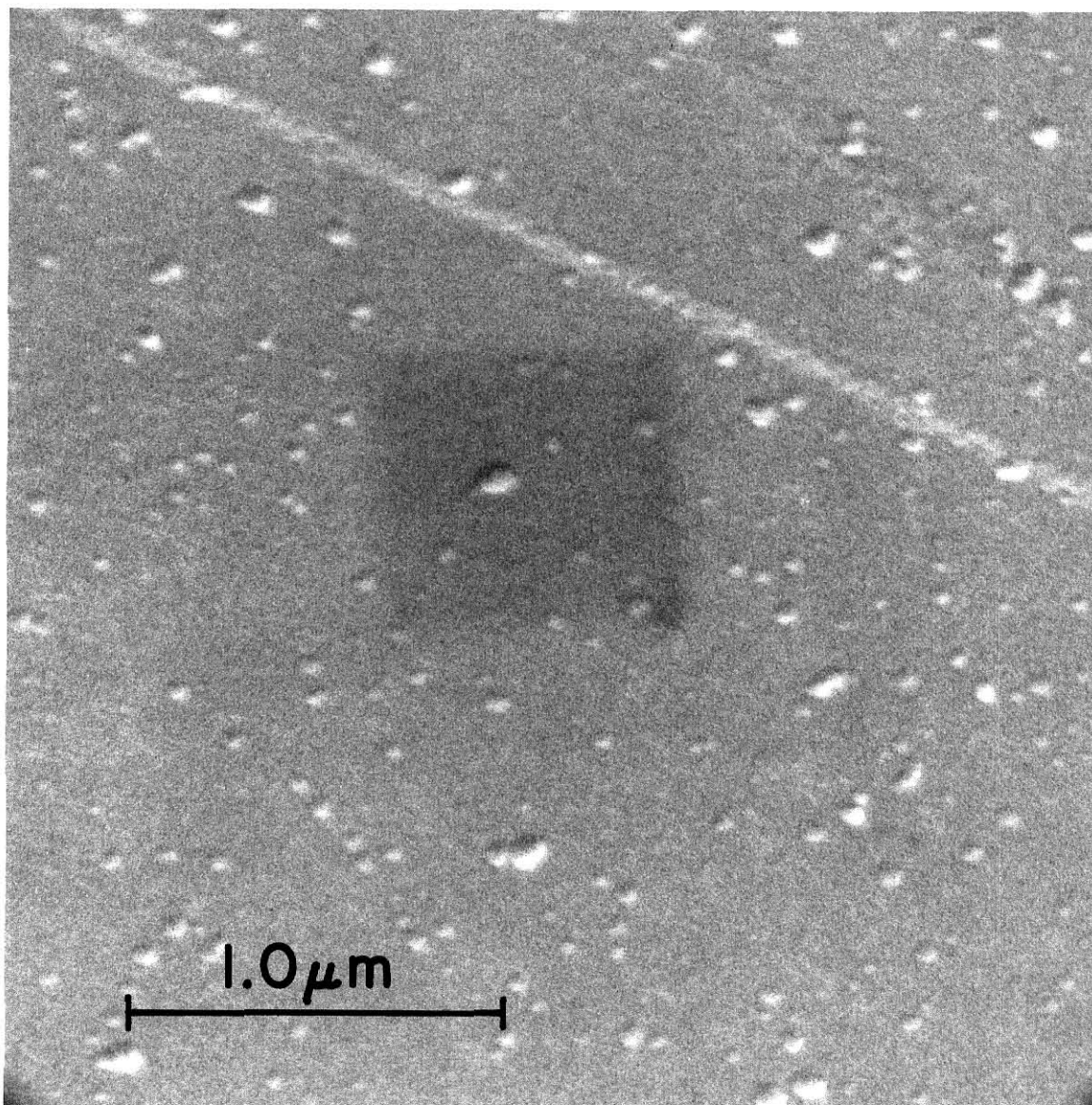


Fig. 14 TLD-100 Treatment: 846 krad exposure

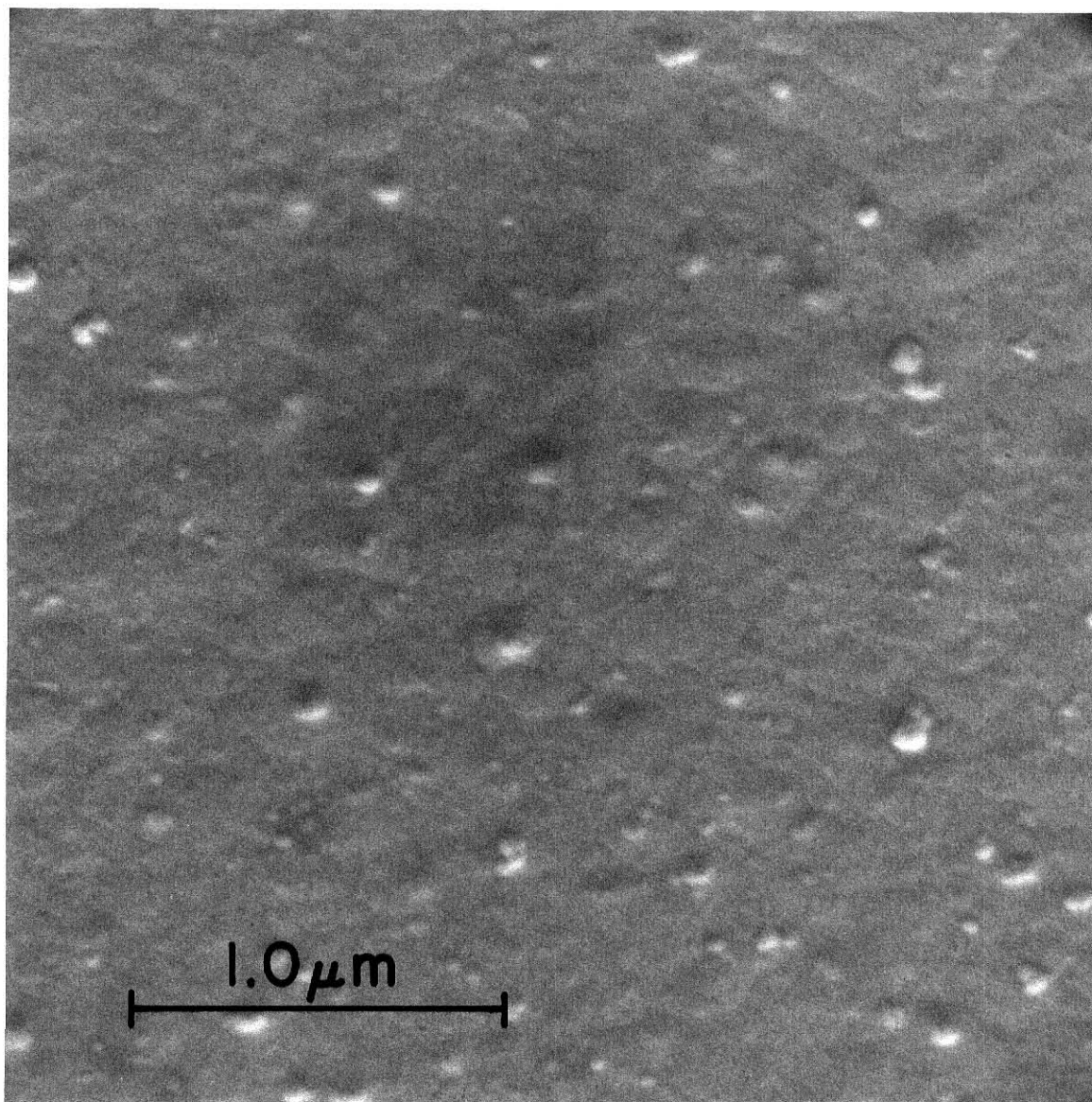


Fig. 15 TLD-100 Treatment: 846 krad exposure, followed by  
24 hrs. at 400°C

## 7. Conclusions

Contrary to the object and direction of this research, Table 1 seems to indicate that an increasing Ti content results in the suppression of peak 2 (7450Å) or the enhancement of peak 1 (4050Å). There are two major factors which have a bearing on these results. Work done by Rossiter, Rees-Evans, and Ellis [16] detected no advantages in the addition of magnesium impurities to LiF above 80 ppm. In the case of the WM-2 crystals, Mg concentrations in the neighborhood of 300 ppm were detected. This seems to indicate that the magnesium in excess of 80 ppm would result in no appreciable increase in the TL output (i.e. concentration quenching). Secondly, evidence in figures 11 and 12 points to the existence of an inhomogeneous distribution of the doping agents ( $\text{MgF}_2$  and/or  $\text{TiF}_3$ ). This would also lead to a smaller light output per ppm of dopant. It is conceivable that these two factors could change the results of the readout process sufficiently to indicate the behavior shown in Table 1.

The only positive results that can be deduced from Table 1 are brought into the light by consideration of individual dopant concentrations. The WM-2 crystals exhibited an extremely small but noticeable increase in the peak ratio. This is coupled with the fact that this group of crystals had a titanium concentration much larger than in the cases of TLD-100 and WM-1. These results, although inconclusive, compare favorably to the results obtained by the three previously mentioned experimenters. They reached the conclusion that titanium acts as an activator (i.e. increases the sensitivity) and that the optimum Ti concentration is about 8 ppm.

The phenomenon of decreasing sensitivity with increasing history was observed and studied. Due to the fact that the actual TL mechanism is not known, the explanation of this entity is difficult. The second series of



micrographs shows the production in the irradiation process and the accentuation in the annealing process of something which is assumed to be responsible for this loss of sensitivity. Since pure LiF exhibits essentially no thermoluminescence, it is safe to assume that impurities are intimately involved with the TL mechanism. Following this line of thought, it would be logical to assume that a loss in sensitivity would be related to a phenomenon which somehow affects the impurities present. Consequently, there seems to be the possibility that the clustering of the fine grain structure seen in figures 14 and 15 was the aggregation of impurities. The aggregation of impurities has previously been observed as an effect caused by certain annealing temperatures and cooling rates. Johnston [17] has reported the formation of aggregates of the impurities in TLD-100 when slow cooling was employed. He has stated that the temperature range from 100 to 200°C is critical. Slow cooling in this range serves to "purify" the LiF lattice by the precipitation of excess magnesium, sometimes in the form of  $MgF_2$ . Since impurities appear to act as trapping or recombination centers, their inhomogeneous distribution would result in a smaller probability of TL transitions.

It appears that there is still much to be learned about thermoluminescence. If better quality crystals of various dopant concentrations could be obtained, it would be worthwhile to repeat this research in greater detail. Also deserving of further investigations is the phenomenon of decreasing sensitivity.

## 8. Acknowledgements

The author wishes to thank the many people who have contributed significantly to the completion of this work: Dr. Donnert and Dr. Merklin, for lending guidance and direction; Bill Starr, for his troubleshooting of experimental equipment; and to the Nuclear Engineering Department, whose grant of an assistantship to the author helped provide the financial support necessary.

The author will be eternally indebted to his father and late mother for their love, encouragement, and confidence in him which was invaluable in times of difficulty.

Last but not least, the author would like to acknowledge the love and devotion of his wife, who has worked both at home and at various jobs for many years to make this work possible.

## 9. References

1. F. Daniels, C. A. Boyd and D. F. Saunders, Science 117, 343 (1953)
2. Kaiseruddin, M., "Spectral Analysis of  $^6\text{LiF:Mg}$  Thermoluminescent Samples," Ph. D. Dissertation, Kansas State University, 1973.
3. Nelson, W., "Area Photoconductivity in Lithium Fluoride," M. S. Thesis, Kansas State University, 1974.
4. Mehta, S., "Study of Optical Absorption Bands Responsible for Thermoluminescence of  $\text{LiF:Mg}$ ," Ph.D. Dissertation, Kansas State University, 1972.
5. Kaiseruddin, M., "Effects of Very High Dose Rates on the Response of  $\text{LiF}$  Thermoluminescent Dosimeters," M. S. Thesis, Kansas State University, 1968.
6. Kan, C., "The Response of  $\text{CaF}_2\text{:Mn}$  Thermoluminescent Dosimeters to Neutrons from a  $^{252}\text{Cf}$  Source," M. S. Thesis, Kansas State University, 1973.
7. Khanna, N., "Thermoluminescent Response of  $\text{LiF:Mg}$  to Gamma and Neutron Radiation," M. S. Thesis, Kansas State University, 1973.
8. Bliss, C., "The Response of  $^6\text{LiF}$  and  $^7\text{LiF}$  Thermoluminescent Dosimeters to Neutron and Gamma Radiation Dose," M. S. Thesis, Kansas State University, 1969.
9. Alexander, A., "The Response Characteristics of  $\text{CaF}_2\text{:Mn}$  Thermoluminescent Dosimeters," M. S. Thesis, Kansas State University, 1970.
10. Laudise, The Growth of Single Crystals, Prentice-Hall, Englewood Cliffs, New Jersey.
11. Installation and Operation Instruction for N.R.C. Type 2801C Crystal Growing Furnace, N.R.C. Equipment Corporation, Newton Highlands, Massachusetts.
12. Operation and Maintenance Instructions for Silicon Rod Growers, Western Electric Company, Inc., Kansas City, Missouri.
13. Thermoluminescent Dosimeter System, Programmer Model 2010A, EG & G Technical Manual Number B-4302, 1970.
14. Instruction Manual, 82-40 .25 Meter Ebert Monochromator, Jarrel-Ash Company, Waltham, Massachusetts.
15. Gilman, J. J. and Johnston, W. G., J. Appl. Phys. 29, 877 (1958)



16. Rossiter, M. J., D. B. Rees-Evans and S. C. Ellis, "Impurities and Thermoluminescence in Lithium Fluoride," Proceedings of the Third International Conference on Luminescence Dosimetry, 1971.
17. Johnston, W. G., J. Appl. Phys. 33, 2050 (1962)

EFFECT OF DOPANT CONCENTRATION ON THE  
THERMOLUMINESCENT RESPONSE OF LiF

by

WILLIAM A. MORRISON

B.S., Grove City College, 1973

---

AN ABSTRACT OF A MASTER'S THESIS

submitted in partial fulfillment of the  
requirements for the degree

MASTER OF SCIENCE

Department of Nuclear Engineering

KANSAS STATE UNIVERSITY  
Manhattan, Kansas

1975

### Abstract

By employing the Czochralski technique, single crystals of lithium fluoride were grown. The dopant concentration of titanium and magnesium were varied. The effect of these major impurities on the two peaks in the TL spectrum was studied. The initial intent of this work was to determine if a relationship existed between the ratio of the dopant concentrations and the ratio of the areas under the two peaks (i.e. 7450 and 4050Å) in the thermoluminescence spectrum. Experimental results were inconclusive at best, probably due to poor quality crystals obtained from the growth process. There was a slight increase in the 7450Å peak when the Ti content was increased significantly. Also observed was a decrease in sensitivity in both commercial and "home-grown" crystals with increasing history. With the use of a scanning electron microscope, micrographs were obtained which pointed to the possibility of impurity aggregation resultant from gamma irradiation and accentuated by the annealing treatment.